Hindawi Publishing Corporation
Advances in Optical Technologies
Volume 2015, Article ID 837183, 8 pages
http://dx.doi.org/10.1155/2015/837183

Research Article

A Comparison of Different A-, A-B-, and B-Site Incorporated in $(Ba_{0.5}Sr_{0.5})TiO_3$ on Photocatalytic Application

Tassanee Tubchareon, Rachan Klaysri, and Piyasan Praserthdam

Center of Excellence on Catalysis and Catalytic Reaction Engineering, Department of Chemical Engineering, Faculty of Engineering, Chulalongkorn University, Bangkok 10330, Thailand

Correspondence should be addressed to Piyasan Praserthdam; piyasan.p@chula.ac.th

Received 1 September 2015; Revised 17 October 2015; Accepted 16 November 2015

Academic Editor: Mikhail Noginov

The structural modification of $Ba_{0.5}Sr_{0.5}TiO_3$ (BST) nanocatalyst was successfully synthesized via sol-gel process. The BST catalyst was modified by A-site (A-BST), A-B-site (A-B-BST), and B-site (B-BST) in order to investigate the effect of structurally modified BST catalyst for photocatalytic decolorization of methylene blue. The structurally modified BST catalysts can increase the nonradiation energy such as phonon energy compared to that of BST one. The partial incorporation of the A-BST catalyst was evidenced by the higher-ordered structure by increasing number of Ti^{4+} ions and the lattice oxygen. The A-B-BST and A-BST catalysts were given more electron-transfer in the TiO_6 than that of BST and B-BST catalysts, respectively. The A-B-BST catalyst promoted the oxidation of the lattice oxygen by holes capturing to form the chemisorbed oxygen, presenting the highest photobleaching activity of methylene blue. On the other hand, more oxygen vacancies recombination of BST catalyst compared to that of structurally modified BST catalysts presented the reduction of photocatalytic activity.

1. Introduction

Perovskite-oxides have been extensively studied due to their excellence in electrical [1] and optical properties [2, 3]. Recently, perovskite-oxides have attracted great interest in their use as nanocatalysts in the photocatalytic decolorization of methylene blue applications such as $BaTiO_3$ [4], $SrTiO_3$ [4, 5], $CaTiO_3$ [4, 6, 7], and $Ba_{1-x}Sr_xTiO_3$ [8].

Both lighting and catalysis are especially for photoreactions. The electron-hole pairs are generated by light absorption which forms the catalytically active species. The partial electron-hole can be recombined, causing the defect chemistry, that is, V_O^Z and V_{Ti}^X. The photogenerated charge carriers can easily reach the surface before their recombination. The electron can be absorbed and reacted with oxygen molecule by reduction process in conduction band, while the hole can be oxidized with water and the other products via the oxidation process in valence band. Recently, the optical property such as photoluminescence (PL) has attentively demonstrated defect structures of perovskite [9–12]. Moreover, PL spectra can also determine a possible mechanism of radiative transition within band gap energy [13, 14]. In our previous work, we reported the representative metal-doped BST powders [13]. The balance of vacancy sites was created in crystalline by charge compensation process leading to electron charge neutrality. The electron-transfer in the TiO_6 is observed in violet emissions. Moreover, the recombination process is involved by oxygen vacancies $[V_O^Z]$ resulting in charge compensation process which appeared in green emissions. It is well known that the point defects, charge transfer, metal-doping, impurity, and/or oxygen activity play the essential roles in photocatalytic process [15]. Generally, the predominant charge compensation process for acceptor-type dopants created the oxygen vacancies, thus changing the electronic structure. In order to well understand the point defects and the electronic structure of the structurally modified BST catalysts, this work aims to study the importance of structurally modified A-site, A-B-site, and B-site of BST catalysts that related electronic structure, point defects, and photocatalytic decolorization of methylene blue.

2. Experimental

2.1. Material Synthesis. All starting materials in this work were commercially available and were used without further purification. The sodium hydroxide [NaOH, 99% Merck] was employed as solute addition in A-site modified BST catalyst, whereas B-site doped BST catalyst was used with ethanol [C_2H_5OH, 99.9% Merck] as solvent addition. The nomenclature in this work defines as X-BST, where X is a site of metal that substituted in BST. Barium hydroxide octahydrate [$Ba(OH)_2{\cdot}8H_2O$, 98% Aldrich], strontium nitrate [$Sr(NO_3)_2$, 99% Aldrich], and titanium (IV) isopropoxide [$C_{12}H_{28}O_4Ti$, 97% Aldrich] were used as Ba, Sr, and Ti precursors, respectively. The starting solution (50 mL) contained the (Ba + Sr) metallic and Ti metallic, at (Ba + Sr)/Ti ratio that was 1, whereas the ratio of Ba/Sr is equal to 0.5.

The BST and all structurally modified BST catalysts were synthesized by mean of sol-gel process. Barium hydroxide octahydrate, strontium nitrate, and A-site modified precursor were dissolved in deionized water. For B-site and A-B-site modified BST catalysts, their modified precursors were dissolved in ethanol solvent. The solution was stirred for one hour at mild heating in order to completely dissolve all metallic precursors. The solution was left to stir at room temperature for 2 h, and then titanium (IV) isopropoxide was added drop wise and continuously stirred until appearing white precipitates. The solution was then stirred overnight at room temperature in order to complete mixing. The solution was washed three times in methanol, and as-synthesized BST powder was dried in the oven at 110°C and finally calcined in stagnant air at 750°C for 5 hours.

2.2. Material Characterizations. All samples characterizations were examined at room temperature. The catalysts were characterized by XRD, XPS, PL, UV-Vis, and EPR. The X-ray diffraction (XRD) was examined by SEIMENS D5000 with CuKα and Ni filter. The X-ray photoelectron spectroscopy (XPS) was measured by AMICUS using MgKα X-ray source. The C *1s* was used as the reference peak at 285.0 eV. The PL measurement was performed by using Perkin Elmer LS 55 and the PL spectra were excited by Xenon lamp at 325 nm. The ultraviolet-visible spectroscopy (UV-Vis) was evaluated with VARIAN CARY 5000 instrument. The electron paramagnetic resonance (EPR) was determined by JEOL model JES-RE2X with the use of DPPH for g-value (g = 2.0036) calibration.

2.3. Methylene Blue Photobleaching. The 200 mL of 4×10^{-5} M of methylene blue aqueous solution and 30 mg of catalyst were introduced into the reactor. The degradation was carried out at room temperature. The suspension was firstly stirred in the dark for 30 minutes before UV (Philips TUV 16W SE UNP) light irradiations to attain absorption-desorption equilibrium on the catalyst surface. The methylene blue photobleaching was evaluated based on the adsorption of UV-Vis spectra at the wavenumber 665 nm. The percentage of photodegradation was calculated by $[(C_0 - C_t) \times 100]/C_0$, where C_0 was the initial concentration of methylene blue and C_t was the concentration of methylene blue at time t.

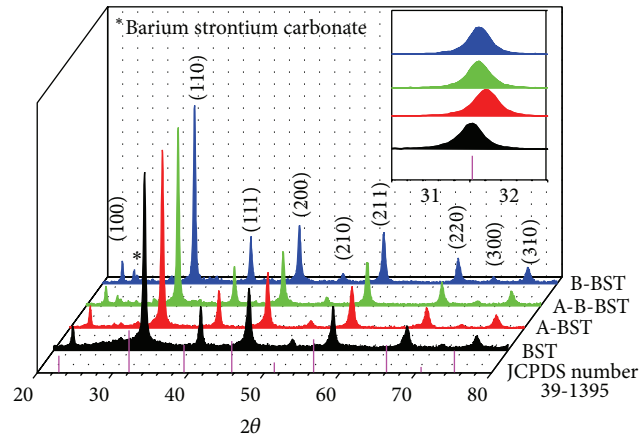

FIGURE 1: The diffraction patterns of BST catalysts.

3. Results and Discussions

The XRD patterns of all $Ba_{0.5}Sr_{0.5}TiO_3$ (BST) catalysts which were treated in stagnant air at 750°C for 5 hours are illustrated in Figure 1. The diffraction peaks of BST, A-B-BST, and B-BST catalysts presented the cubic structural of BST crystalline which referred to Joint Committee on Powder Diffraction Standards (JCPDS) number 39-1395 while the A-BST catalyst appeared as a slightly asymmetrical diffraction peak of (200) located in the range of 44–47° resulting in the occurrence of the tetragonal structure. The tetragonality (c/a ratio) of the A-BST catalyst was 1.004. The diffraction peaks that shifted from the BST one can be implying the partial substitution of metal-dopant occurring in $Ba_{0.5}Sr_{0.5}TiO_3$ structure. The ionic radii of metal-doped BST moderately affected the lattice parameter, whereas there was an insignificant difference in crystallite size, as per the results that were provided in Table 1. The results revealed that A-site or Ba^{2+}/Sr^{2+} ions are partially substituted by smaller ionic radii of Na^+ [$Na'_{Ba/Sr}$], thus decreasing in lattice parameter. For the C^{4+} ions, they can be inserted into all A-sites, B-sites (Ti^{4+}), and O^{2-}. However, the C^{4+} ions are preferentially substituted into B-site or Ti^{4+} [16, 17] because of the low energy formation required [16]. Moreover, the C^{4+} ions partially occupied B-sites [$C_{Ti}{}^X$] which were clearly confirmed by the residual carbonate ($BaSrCO_3$) formation in BST lattice and a slight shifting of XRD peaks toward the higher angle. The $BaSrCO_3$ exhibited a small diffraction peak at ca. 24°.

The incorporation of metal into BST crystalline not only changed the lattice parameter but also particularly affected a structural defect. The ordered structure of titanate-based perovskite can be determined from [TiO_6-TiO_{6-x}] clusters, in which A-/B- cations and their vacant sites are arranged in order that is close to the perfect crystalline. These clusters are noteworthy when the A- or B-site vacancies are absent. The disordered structure can suggest that the metal-dopant is randomly distributed in the perovskite structure which can be explained as [TiO_5-$V_O{}^Z$-TiO_6] clusters. The oxygen vacancies [$V_O{}^Z$] can possibly appear in three states: (i) neutral oxygen vacancy [$V_O{}^X$]; (ii) singly ionized oxygen

Table 1: Phase structure, crystallite size, and lattice parameters of BST and the structural modified BST catalysts.

Sample	Phase	Crystalline size[1] (nm)	Lattice parameter (nm)[1]		
			a	c	c/a
BST	Cubic	30	0.3954	—	—
A-BST	Tetragonal	30	0.3931	0.3946	1.004
A-B-BST	Cubic	28	0.3941	—	—
B-BST	Cubic	27	0.3941	—	—

[1]The cubic phase was calculated from Bragg's law using the diffraction peaks of (110) so the tetragonal phase uses the diffraction peaks of (110) and (111).

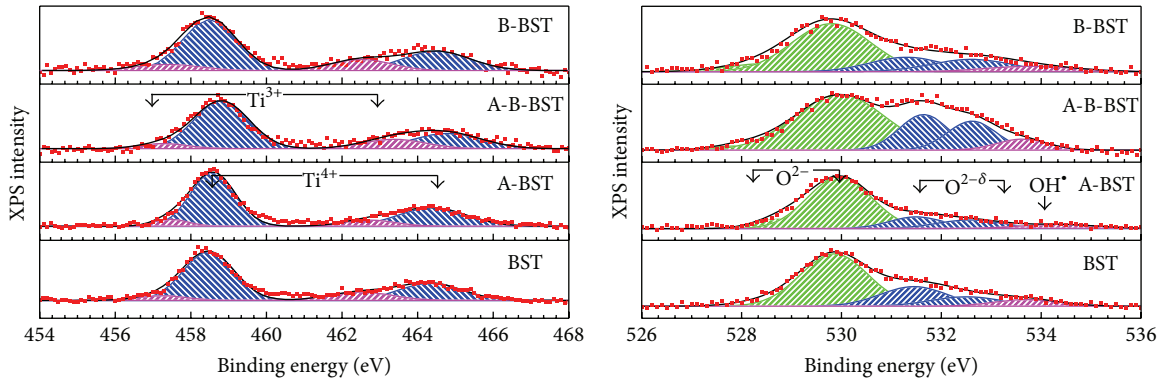

Figure 2: XPS spectra of BST catalysts (a) Ti *2p* and (b) O *1s*.

Table 2: Surface atomic percentage of Ti *2p* and O *1s* of BST and modified BST catalysts.

Sample	Surface atomic concentration of Ti *2p* (%)		Surface atomic concentration of O *1s* (%)		
	Ti^{3+}	Ti^{4+}	O^{2-}	$O^{2-\delta}$	$O_{OH}^{\bullet}$
BST	17.95	82.05	64.48	29.34	6.18
A-BST	13.01	86.99	71.21	22.68	6.12
A-B-BST	18.59	81.41	58.65	35.17	6.19
B-BST	20.75	79.25	64.07	29.02	6.92

vacancy [$V_O^{\bullet}$]; and (iii) fully ionized oxygen vacancy [$V_O^{\bullet\bullet}$] [18].

Figure 2(a) illustrates the defect spectra of [TiO_5-V_O^Z] clusters or Ti^{3+} species which can be found at 457.5 eV and 462.5 eV, while the presence of TiO_6 clusters or Ti^{4+} species exhibited the peaks at 458.5 and 464.4 eV [19, 20]. The surface atomic percentage of Ti *2p* is provided in Table 2.

The surface atomic percentage of Ti^{4+} in BST increased in the order of A-BST > BST > A-B-BST > B-BST. This result agreed well with the EPR result, as shown in Figure 3. It can be clearly seen that the BST catalyst presented the highest intensity of a symmetric signal of g-value about 2.004. The intensity of g-value of A-B-BST, B-BST, and BST catalysts was more than that of A-BST catalyst. This signal was ascribed to the singly ionized [TiO_5-$V_O^{\bullet}$] [21, 22]. Moreover, the BST catalyst exhibited slight peaks of g-value ca. 1.973 and 2.030. These peaks were attributed to barium vacancies [V'_{Ba}] [23, 24] and oxygen radicals [$O_x^{-\bullet}$] [25], respectively. The occurrence of Ti^{3+} species in structure implied that the free electron/hole may be transferred in the lattice and may have formed the oxygen chemisorption species. The deconvolution of O *1s* is represented in Figure 2(b). The first species demonstrated at ca. 528.7 and 529.8 eV [26–28] can be attributed to the lattice oxygen (O_L or O^{2-}). Secondly, the chemisorbed oxygen (O_C or $O^{2-\delta}$) appeared at 531.4 and 532.4 eV [26, 27]. For the last one, the oxygen in hydroxyl radical ($O_{OH}^{\bullet}$) was observed at 533.5 eV [27].

In order to maintain electroneutrality of partial Ba^{2+}/Sr^{2+} substituted by Na^+ in lattice, the charges compensated either by the hole formation (1) and/or by the creation of oxygen vacancy (2) are given below:

$$\text{BST} \xleftrightarrow{Na^+} Na'_{Ba/Sr} + h^{\bullet} + \text{BST} \quad (1)$$

$$\text{BST} \xleftrightarrow{Na^+} Na'_{Ba/Sr} + V_O^Z + \text{BST} \quad (2)$$

whereas

$$V_O^{\bullet\bullet} \xleftrightarrow{e^-} V_O^{\bullet} \xleftrightarrow{e^-} V_O^X \quad (3)$$

The result revealed that the partial incorporation of [$Na'_{Ba/Sr}$] did not only improve the amount of Ti^{4+} in crystalline by Ti^{3+} oxidation as in (4) but also enhance

Table 3: Indirect band gap, phonon energy, and percentage of PL emissions of BST catalysts.

Sample	Indirect band gap (eV)	Phonon emissions energy (eV)	Phonon absorption energy (meV)	Nonradiative energy (eV)	PL emissions (%)					
					Violet		Blue	Green		Yellow
					≈3.16	≈2.95	≈2.76 (eV)	≈2.55	≈2.35	≈1.94
BST	3.10	0.66	60.26	0.72	32.83	18.85	17.19	10.49	12.17	8.46
A-BST	3.06	0.66	61.72	0.72	30.76	27.21	21.92	12.50	5.29	2.32
A-B-BST	3.10	0.68	86.71	0.77	25.55	27.72	24.13	14.36	5.53	2.71
B-BST	3.05	0.62	135.77	0.76	27.77	14.06	28.53	11.10	7.43	9.11

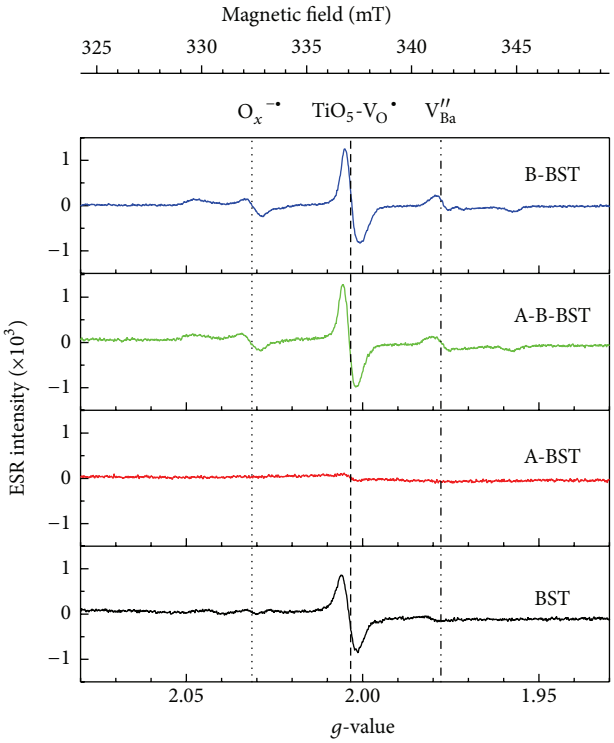

Figure 3: EPR spectra of BST catalysts.

the reduction of the chemisorbed oxygen to the lattice oxygen as in (5). Consider

$$Ti^{3+} + h^{\bullet} \longleftrightarrow Ti^{4+} \quad (4)$$

$$O_2 \longleftrightarrow O_2 \overset{e^-}{\longleftrightarrow} O_2^- \overset{e^-}{\longleftrightarrow} O_2^{2-} \overset{e^-}{\longleftrightarrow} 2O^- \overset{2e^-}{\longleftrightarrow} 2O^{2-} \quad \text{(lattice)} \quad (5)$$

The partial substitution of Ti^{4+} by C^{4+} species in the crystalline did not require the charge compensation. However, some oxide species appeared to lose oxygen and became nonstoichiometric defect in the sense of oxygen-deficiency when heated in atmosphere such as air: TiO_2 is an example. This result shows a slightly changed surface concentration of O *1s*. In addition, free electron occurring as a result of nonstoichiometric defect can form the partial reduction of Ti^{4+} to Ti^{3+} specie. However, the partial incorporation of $[Na'_{Ba/Sr}]$ and $[C_{Ti}{}^{X}]$ in BST lattice plays an essential role in promoting the oxidation of the lattice oxygen to the chemisorbed oxygen. According to this result, it can be suggested that the lattice oxygen may partially capture holes leading to increasing of the chemisorbed oxygen in crystalline. The chemisorption of oxygen species is important in photocatalysis for water purification [15].

The disordered structure appears as a vacancy defect that can produce electron and hole charge compensation within band gap. Generally, the band gap of titanate-perovskite is different in energy level between O *2p* orbitals in valence band and Ti *3d* orbitals in conduction band. The possible model of radiative transitions of BST is proposed in Figure 4.

Electrons are excited from valence band maximum (VB_{max}) to the conduction band minimum (CB_{min}) by light/photon emissions. During the excitation ca. 3.82 eV at room temperature, an excited electron can decay either radiatively by emitting a photon or nonradiatively by its transforming excitation energy entirely into heat or phonon [29]. In general, the luminescence energy is lower than the optical absorption energy on account of the thermalization of phonon emissions that is called a Stokes shift [30, 31]. As a result in Table 3, the nonradiative energy of structurally modified BST catalysts was higher than the BST one. A large Stokes shift implied the promoting nonradiative decay and the strong electron-lattice interaction [32, 33].

If such photons have energy higher than band gap, they can be reabsorbed and promoted another electron to the conduction band. Consequently, this stimulus energy induced localization and delocalization process; photon energy is emitted. The photon emissions are determined by the crystal color or color centers as shown in PL behaviors as depicted in Figure 5. The deconvolution of PL spectra for BST and structural modified BST catalysts is given in Figure 5(b) and Table 3. The first peak in range of 3.0–3.1 eV is attributed to indirect band gap energy. This result is in well agreement with UV-Vis result, as illustrated in Figure 6. Figure 6 demonstrates the absorbance spectra of all BST catalysts that substantially decreased in wavelength ca. 370 nm or in photon energy about 3.1 eV. As a result, the structurally modified BST catalysts slightly reduced the indirect band gap values, as contained in Table 3. The second peak around 2.95 eV was assigned to the electron transferring in TiO_6, causing the oxygen vacancies $[V_O{}^{Z}]$ in the structure [34, 35]. The occurrence of charge compensation processes as a result imbalances charge transfer leading to difference in

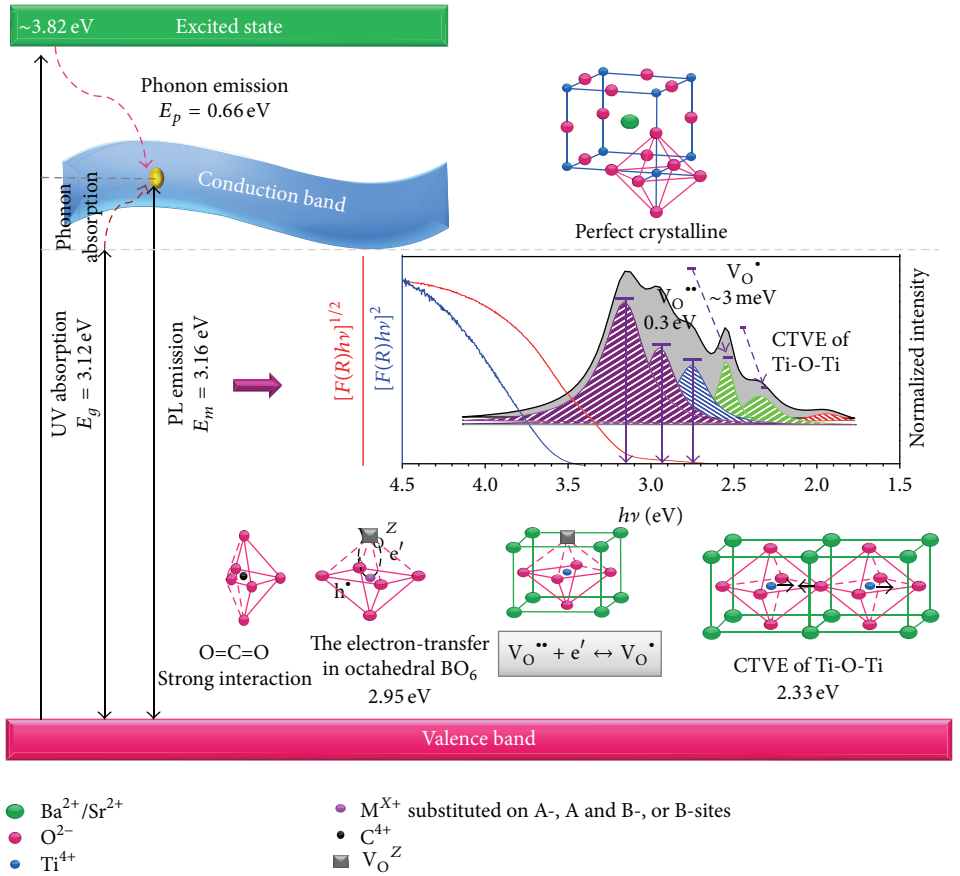

Figure 4: The possible model of radiative transitions of BST catalysts.

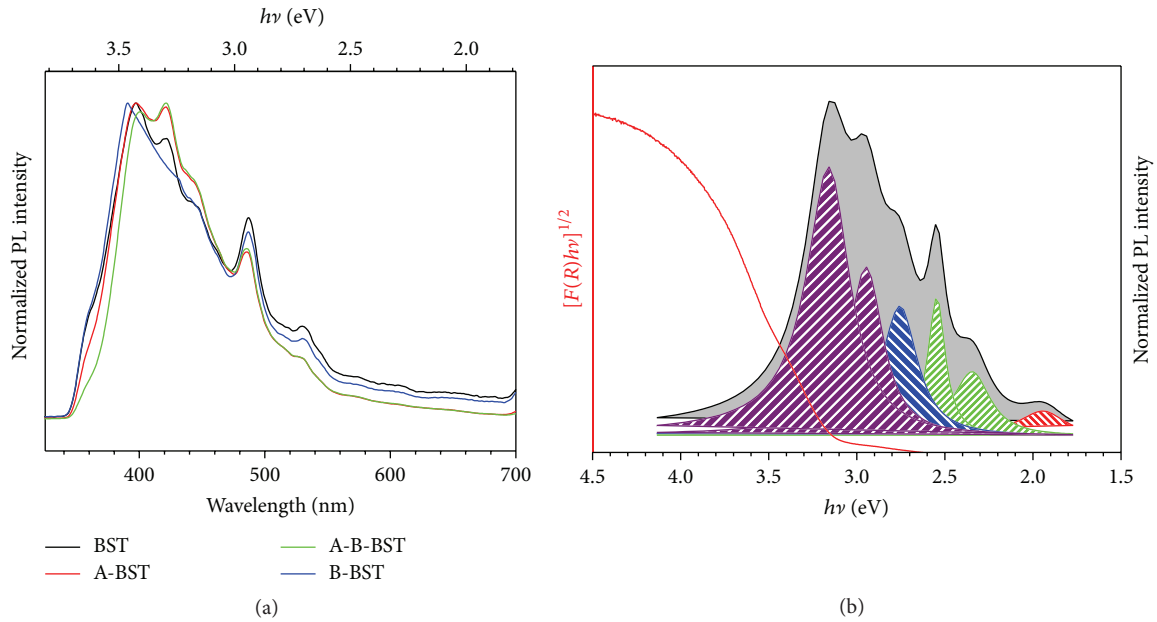

Figure 5: (a) PL spectra of BST, (b) the deconvolution spectra of BST catalysts.

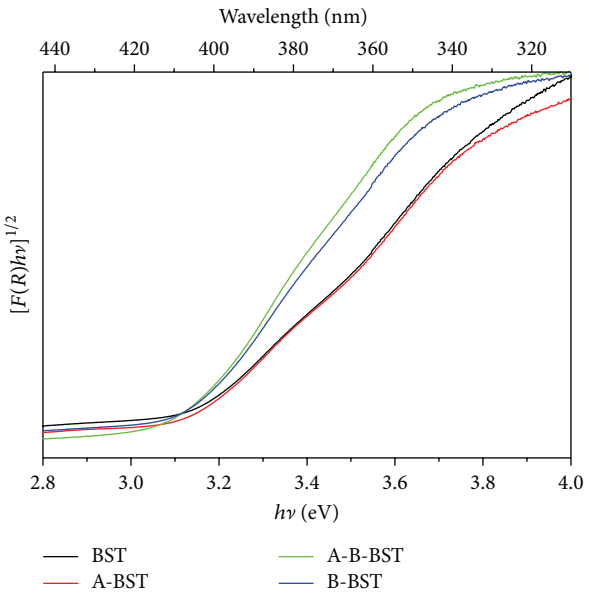

Figure 6: UV-Vis spectra of BST catalysts.

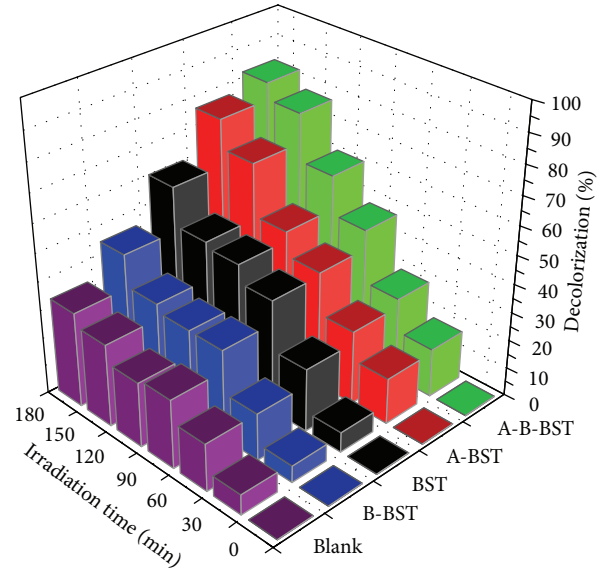

Figure 7: The photobleaching of methylene blue under UV illuminations.

PL intensity [13]. The PL intensity is dependent on electron deficient in TiO_6 clusters in order of A-B-BST ≈ A-BST > BST > B-BST. The partial Na^+ substitution into A-site $[Na'_{Ba/Sr}]$ of BST is deficient in an electron; for example, the deficiency may be viewed as hole that is weakly bound to the impurity atom. The $[Na'_{Ba/Sr}]$ acted as an acceptor impurity that located within the band gap. The acceptor state of $[Na'_{Ba/Sr}]$ is capable of accepting electron from conduction band, leaving behind a hole [36]. The partial substitution of C^{4+} in Ti^{4+}, $[C_{Ti}{}^{X}]$ [17] can suppress the electron movement in O=C=O bond, thus decreasing the electron transfer in B-BST. The oxygen vacancy site acts as an electron donor that can generate electron-hole and simultaneous recombination [37].

The oxygen vacancies could be induced by network structure randomly mixed $[BO_5 \cdots V_O{}^{Z}]$ and $[AO_{11} \cdots O]$ [21, 38]. The charge transfer of fully ionized oxygen vacancy $[V_O{}^{\bullet\bullet}]$ and the singly ionized oxygen vacancy $[V_O{}^{\bullet}]$ is illustrated at 2.80 and 2.55 eV, respectively. Two oxygen vacancy sites are generally exhibited at the positions below conduction band approximately 0.3 eV and 3 meV, respectively [37]. At 2.33 eV, this peak is attributed to the charge-transfer vibronic excitons (CTVE) of Ti-O-Ti bonds [39, 40]. This result agreed well with energy migration arising from $[V_O{}^{X}]$ in bulk $SrTiO_3$ that occurs below the conduction band ca. 0.69 eV [41]. Moreover, the intensity of PL emissions depends on the interaction of complex clusters [35] and number of vacancy sites [14]. The decrease of PL spectra represented that the recombination of oxygen vacancies was in the sequence of A-B-BST ≈ A-BST > B-BST > BST. It is implied that the structurally modified BST structure can suppress the oxygen vacancies recombination.

Figure 7 shows the photobleaching of methylene blue under UV illuminations. The results indicated that the photocatalytic activity of methylene blue increased in the order of B-BST > BST > A-BST > A-B-BST. The results can suggest that the electron-transfer in TiO_6 and the chemisorbed oxygen species were highly significant for photocatalyst decolorization of methylene blue. The A-B-BST and A-BST catalysts were more intense in electron-transfer in TiO_6 (see Figure 5(a)), whereas the chemisorbed oxygen species of A-B-BST was higher than that of A-BST; thus A-B-BST is exhibiting the highest photocatalyst activity. Moreover, the oxygen vacancies recombination of BST catalyst was higher than that of structurally modified BST one (see Figure 5(a)), resulting in less decolorization of methylene blue. Furthermore, the B-BST catalyst was lower photodegradation of methylene blue since the strong interaction of C-O covalent bond suppresses the electron-transfer in TiO_6 [17].

4. Conclusions

The A-site, A-B-site, and B-site structural modification of $Ba_{0.5}Sr_{0.5}TiO_3$ catalysts were investigated. The partial substitution of metal-dopant into BST catalyst was confirmed by the shifting of XRD patterns, thus varying the lattice parameter. The lattice vibration due to the structural modified BST catalysts can increase the nonradiation energy such as phonon energy. The partial incorporation of metal-dopant was significant species of Ti and O in order to maintain charge neutrality in BST structure. However, the indirect band gap energy of structurally modified BST was slightly lower than that of BST. Moreover, the BST catalyst shows more intensity of oxygen vacancies recombination process in PL spectra than ones, thus reducing photocatalytic degradation of methylene blue. The photobleaching activity of methylene blue depends on both the electron-transfer in TiO_6 and the chemisorbed oxygen species. The A-B-BST catalyst was given the highest photocatalytic decolorization of methylene blue, while the B-BST gave the lowest activity due to the strong interaction of C=O bond in TiO_6.

Conflict of Interests

The authors declare that there is no conflict of interests regarding the publication of this paper.

Acknowledgment

This research is supported by Rachadapisek Sompote Fund for Postdoctoral Fellowship, Chulalongkorn University.

References

[1] B. Hou, Y. Xu, D. Wu, and Y. Sun, "Preparation and characterization of single-crystalline barium strontium titanate nanocubes via solvothermal method," *Powder Technology*, vol. 170, no. 1, pp. 26–30, 2006.

[2] F. M. Pontes, E. Longo, E. R. Leite et al., "Photoluminescence at room temperature in amorphous $SrTiO_3$ thin films obtained by chemical solution deposition," *Materials Chemistry and Physics*, vol. 77, no. 2, pp. 598–602, 2003.

[3] F. M. Pontes, C. D. Pinheiro, E. Longo et al., "Theoretical and experimental study on the photoluminescence in $BaTiO_3$ amorphous thin films prepared by the chemical route," *Journal of Luminescence*, vol. 104, no. 3, pp. 175–185, 2003.

[4] S. Otsuka-Yao-Matsuo, T. Omata, S. Ueno, and M. Kita, "Photobleaching of methylene blue aqueous solution sensitized by composite powders of titanium oxide with $SrTiO_3$, $BaTiO_3$, and $CaTiO_3$," *Materials Transactions*, vol. 44, no. 10, pp. 2124–2129, 2003.

[5] T. Tsumura, K. Sogabe, and M. Toyoda, "Preparation of $SrTiO_3$-supported TiO_2 photocatalyst," *Materials Science and Engineering B*, vol. 157, no. 1–3, pp. 113–115, 2009.

[6] H. Yang, C. Han, and X. Xue, "Photocatalytic activity of Fe-doped $CaTiO_3$ under UV-visible light," *Journal of Environmental Sciences*, vol. 26, no. 7, pp. 1489–1495, 2014.

[7] H. Yoshida, L. Zhang, M. Sato et al., "Calcium titanate photocatalyst prepared by a flux method for reduction of carbon dioxide with water," *Catalysis Today*, vol. 251, pp. 132–139, 2015.

[8] A. Bhardwaj, N. V. Burbure, and G. S. Rohrer, "Enhanced photochemical reactivity at the ferroelectric phase transition in $Ba_{1-x}Sr_xTiO_3$," *Journal of the American Ceramic Society*, vol. 93, no. 12, pp. 4129–4134, 2010.

[9] V. M. Longo, L. S. Cavalcante, M. G. S. Costa et al., "First principles calculations on the origin of violet-blue and green light photoluminescence emission in $SrZrO_3$ and $SrTiO_3$ perovskites," *Theoretical Chemistry Accounts*, vol. 124, no. 5-6, pp. 385–394, 2009.

[10] S. K. Rout, L. S. Cavalcante, J. C. Sczancoski et al., "Photoluminescence property of $Ba(Zr_{0.25}Ti_{0.75})O_3$ powders prepared by solid state reaction and polymeric precursor method," *Physica B: Condensed Matter*, vol. 404, no. 20, pp. 3341–3347, 2009.

[11] E. C. Paris, J. W. M. Espinosa, S. de Lazaro et al., "Er^{3+} as marker for order-disorder determination in the $PbTiO_3$ system," *Chemical Physics*, vol. 335, no. 1, pp. 7–14, 2007.

[12] L. S. Cavalcante, J. C. Sczancoski, J. W. M. Espinosa et al., "Intense blue and green photoluminescence emissions at room temperature in barium zirconate powders," *Journal of Alloys and Compounds*, vol. 471, no. 1-2, pp. 253–258, 2009.

[13] T. Tubchareon, S. Soisuwan, S. Ratanathammaphan, and P. Praserthdam, "Effect of Na-, K-, Mg-, and Ga dopants in A/B-sites on the optical band gap and photoluminescence behavior of $[Ba_{0.5}Sr_{0.5}]TiO_3$ powders," *Journal of Luminescence*, vol. 142, pp. 75–80, 2013.

[14] D. Kan, T. Terashima, R. Kanda et al., "Blue-light emission at room temperature from Ar^+-irradiated $SrTiO_3$," *Nature Materials*, vol. 4, no. 11, pp. 816–819, 2005.

[15] M. K. Nowotny, L. R. Sheppard, T. Bak, and J. Nowotny, "Defect chemistry of titanium dioxide. Application of defect engineering in processing of TiO_2-based photocatalysts," *Journal of Physical Chemistry C*, vol. 112, no. 14, pp. 5275–5300, 2008.

[16] N. Li and K. L. Yao, "The electronic and optical properties of carbon-doped $SrTiO_3$: density functional characterization," *AIP Advances*, vol. 2, no. 3, Article ID 032135, 11 pages, 2012.

[17] T. Tubchareon, S. Soisuwan, S. Ratanathammaphan, and P. Praserthdam, "Effect of carbon-dopant on the optical band gap and photoluminescence properties of $[Ba_{0.5}Sr_{0.5}]TiO_3$ powders synthesized by the sol–gel process," *Journal of Luminescence*, vol. 145, pp. 919–924, 2014.

[18] L. S. Cavalcante, N. C. Batista, T. Badapanda et al., "Local electronic structure, optical bandgap and photoluminescence (PL) properties of $Ba(Zr_{0.75}Ti_{0.25})O_3$ powders," *Materials Science in Semiconductor Processing*, vol. 16, no. 3, pp. 1035–1045, 2013.

[19] Y. Song, F. Wang, Z. Jiang, and Y. Zhou, "Effect of $BaTi_4O_9$ fibers on dielectric properties of $0.64BaTi_4O_9+0.36BaPr_2Ti_4O_{12}$ composites," *Ceramics International*, vol. 28, no. 6, pp. 685–688, 2002.

[20] W.-D. Yang, "PZT/PLZT ceramics prepared by hydrolysis and condensation of acetate precursors," *Ceramics International*, vol. 27, no. 4, pp. 373–384, 2001.

[21] A. T. de Figueiredo, V. M. Longo, R. O. da Silva et al., "Structural XANES characterization of $Ca_{0.99}Sm_{0.01}TiO_3$ perovskite and correlation with photoluminescence emission," *Chemical Physics Letters*, vol. 544, pp. 43–48, 2012.

[22] L. S. Cavalcante, V. M. Longo, M. Zampieri et al., "Experimental and theoretical correlation of very intense visible green photoluminescence in $BaZrO_3$ powders," *Journal of Applied Physics*, vol. 103, no. 6, Article ID 063527, 2008.

[23] M. S. Castro, W. Salgueiro, and A. Somoza, "Electron paramagnetic resonance and positron annihilation study of the compensation mechanisms in donor-doped $BaTiO_3$ ceramics," *Journal of Physics and Chemistry of Solids*, vol. 68, no. 7, pp. 1315–1323, 2007.

[24] T. Kolodiazhnyi and A. Petric, "Analysis of point defects in polycrystalline $BaTiO_3$ by electron paramagnetic resonance," *Journal of Physics and Chemistry of Solids*, vol. 64, no. 6, pp. 953–960, 2003.

[25] Y. Nakaoka and Y. Nosaka, "ESR investigation into the effects of heat treatment and crystal structure on radicals produced over irradiated TiO_2 powder," *Journal of Photochemistry and Photobiology A: Chemistry*, vol. 110, no. 3, pp. 299–305, 1997.

[26] X. Zhao, Q. Yang, and J. Cui, "XPS study of surface absorbed oxygen of ABO_3 mixed oxides," *Journal of Rare Earths*, vol. 26, no. 4, pp. 511–514, 2008.

[27] Q. Xu, D.-P. Huang, W. Chen, H. Wang, B.-T. Wang, and R.-Z. Yuan, "X-ray photoelectron spectroscopy investigation on chemical states of oxygen on surfaces of mixed electronic-ionic conducting $La_{0.6}Sr_{0.4}Co_{1-y}Fe_yO_3$ ceramics," *Applied Surface Science*, vol. 228, no. 1–4, pp. 110–114, 2004.

[28] N. A. Merino, B. P. Barbero, P. Eloy, and L. E. Cadús, "$La_{1-x}Ca_xCoO_3$ perovskite-type oxides: identification of the surface oxygen species by XPS," *Applied Surface Science*, vol. 253, no. 3, pp. 1489–1493, 2006.

[29] L. Bergman and J. L. McHale, *Handbook of Luminescent Semiconductor Materials*, CRC Press, 2011.

[30] B. Ullrich, D. Ariza-Flores, and M. Bhowmick, "Intrinsic photoluminescence Stokes shift in semiconductors demonstrated by thin-film CdS formed with pulsed-laser deposition," *Thin Solid Films*, vol. 558, pp. 24–26, 2014.

[31] M. Lannoo, C. Delerue, and G. Allan, "Theory of radiative and nonradiative transitions for semiconductor nanocrystals," *Journal of Luminescence*, vol. 70, no. 1–6, pp. 170–184, 1996.

[32] W. F. Zhang, J. Tang, and J. Ye, "Photoluminescence and photocatalytic properties of $SrSnO_3$ perovskite," *Chemical Physics Letters*, vol. 418, no. 1–3, pp. 174–178, 2006.

[33] A. A. P. Mansur, F. P. Ramanery, and H. S. Mansur, "Water-soluble quantum dot/carboxylic-poly (vinyl alcohol) conjugates: Insights into the roles of nanointerfaces and defects toward enhancing photoluminescence behavior," *Materials Chemistry and Physics*, vol. 141, no. 1, pp. 223–233, 2013.

[34] P. Bomlai, N. Sirikulrat, and T. Tunkasiri, "Effect of heating rate on the properties of Sb and Mn-doped barium strontium titanate PTCR ceramics," *Materials Letters*, vol. 59, no. 1, pp. 118–122, 2005.

[35] V. M. Longo, A. T. de Figueiredo, S. de Lázaro et al., "Structural conditions that leads to photoluminescence emission in $SrTiO_3$: an experimental and theoretical approach," *Journal of Applied Physics*, vol. 104, no. 2, Article ID 023515, 2008.

[36] W. D. Callister, *Fundamentals of Materials Science and Engineering: An Integrated Approach*, John Wiley & Sons, 2005.

[37] R. Moos and K. H. Härdtl, "Defect chemistry of donor-doped and undoped strontium titanate ceramics between 1000° and 1400°C," *Journal of the American Ceramic Society*, vol. 80, no. 10, pp. 2549–2562, 1997.

[38] A. E. Souza, R. A. Silva, G. T. A. Santos et al., "Order-disorder degree of self-assembled clusters: influence on photoluminescence emission and morphology of $Ba_xSr_{1-x}TiO_3$ nanocrystals," *Chemical Physics Letters*, vol. 514, no. 4–6, pp. 301–306, 2011.

[39] D. Li, H. Haneda, S. Hishita, and N. Ohashi, "Visible-light-driven N-F-codoped TiO_2 photocatalysts. 2. Optical characterization, photocatalysis, and potential application to air purification," *Chemistry of Materials*, vol. 17, no. 10, pp. 2596–2602, 2005.

[40] K.-H. Yang, T.-Y. Chen, N.-J. Ho, and H.-Y. Lu, "In-gap states in wide-band-gap $SrTiO_3$ analyzed by cathodoluminescence," *Journal of the American Ceramic Society*, vol. 94, no. 6, pp. 1811–1816, 2011.

[41] Y. F. Zhukovskii, E. A. Kotomin, S. Piskunov, Y. A. Mastrikov, and D. E. Ellis, "The effect of oxygen vacancies on the atomic and electronic structure of cubic ABO_3 perovskite bulk and the (001) surface: *Ab* initio calculations," *Ferroelectrics*, vol. 379, no. 1, pp. 191–198, 2009.